European Journal of Medicinal Chemistry 80 (2014) 83–91

Contents lists available at ScienceDirect

European Journal of Medicinal Chemistry

journal homepage: http://www.elsevier.com/locate/ejmech

Short communication

Synthesis, cytotoxic study and docking based multidrug resistance modulator potential analysis of 2-(9-oxoacridin-10(9*H*)-*yl*)-N-phenyl acetamides

Rajesh Kumar [a,b], Maninder Kaur [b], Malkeet Singh Bahia [b], Om Silakari [b,*]

[a] Pharmaceutical Chemistry Division, Shivalik College of Pharmacy, Nangal, Punjab 140126, India
[b] Molecular Modeling Lab (MML), Department of Pharmaceutical Sciences and Drug Research, Punjabi University, Patiala, Punjab 147002, India

ARTICLE INFO

Article history:
Received 17 August 2013
Received in revised form
7 April 2014
Accepted 8 April 2014
Available online 12 April 2014

Keywords:
Acridone derivatives
Cytotoxicity
Docking analysis
MTT assay
Multidrug resistance

ABSTRACT

The present study describes the synthesis of fifteen 2-(9-oxoacridin-10(9*H*)-*yl*)-N-phenyl acetamide derivatives (**13a**–**o**) through condensation of 2-chloro-N-phenyl acetamides (**12a**–**o**) with acridone molecule (**10**). All the synthesized compounds were screened for their anti-cancer activity against three diverse cell lines including breast (MCF-7), cervical (HeLa) and lung adenocarcinoma (A-549) employing standard MTT assay. Among synthesized molecules, **13k** and **13l** showed good cytotoxicity activity against considered three cancer cell lines. Additionally, *in silico* studies of multidrug resistance modulator (MDR) effects of these compounds was performed by docking simulation in the ATP binding site of P-gp. The results of docking simulation displayed important interactions of these molecules in the active site of this protein and predicted their MDR modulator behavior.

© 2014 Elsevier Masson SAS. All rights reserved.

1. Introduction

Cancer is a malignant and abnormal cell growth caused by the unspecific division of normal cells. Cancerous cells may invade within the nearby tissues and spread into various parts of the body through the lymphatic or blood system. At present, it has become the leading health hazard, second to cardiovascular complications, which affects the majority of the population worldwide [1]. In the literature, a wide variety of anti-cancer agents have been described for the treatment of various kinds of cancers, however they face the major failure attributed to the development of multi-drug resistance (MDR). Thus, it is a major challenge to the pharmaceutical industry, since the development of MDR limits the use of anti-cancer agents in chemotherapy, *eg.* vinca alkaloids (vincristine, vinblastine), taxanes (paclitaxel), epipodophyllotoxins (etoposide, teniposide) and the topoisomerase inhibitors (topotecan) [2–5]. Therefore, the development of potent and safe anti-cancer agents, which are devoid of MDR or simultaneously modifies the MDR, is a crucial aspect of modern cancer research.

The wide biological potential of naturally occurring lead molecules have always been considered as promising aspect, and researchers are indulged in the development of their molecular libraries [6–8]. In 1948, an acridone alkaloid, acronycine (**1**) was isolated from a *Acronychia baueri* Schott plant belonging to Rutaceae family, which displayed a broad spectrum activity against a variety of experimental tumor models including sarcoma, myeloma, carcinoma, and melanoma [9]. Similarly, Glyfoline (**2**) is an another naturally occurring acridone alkaloid in *Glycosmis citrifolia*, which described high *in vitro* potency to inhibit the cellular growth of human leukemia HL-60 cells [10]. Moreover, an exhaustive research has been conducted on acridine and acridone derivatives showing anti-cancer potential [11–13], and this activity is observed to be mediated through the binding or intercalation of these molecules with DNA of cancer cells [14,15]. The acridine and acridone molecules bearing a planar and tricyclic molecular structure which target the cancer cell DNA by intercalating between nucleotide base pairs in the helix. Many molecules of acridine chemical classes have been used clinically or are under clinical observations, such as amsacrine (**3**), nitracrine (**4**), asulacrine (**5**) and DACA (**6**) (Fig. 1) [11–14,16,17]. The major end product of acridine derivatives is acridone [18], thus a variety of acridone derivatives have been developed and tested for their anti-cancer activity, such as triazoloacridone [19] and

* Corresponding author.
E-mail addresses: omsilakari@rediffmail.com, omsilakari@gmail.com (O. Silakari).

http://dx.doi.org/10.1016/j.ejmech.2014.04.030
0223-5234/© 2014 Elsevier Masson SAS. All rights reserved.

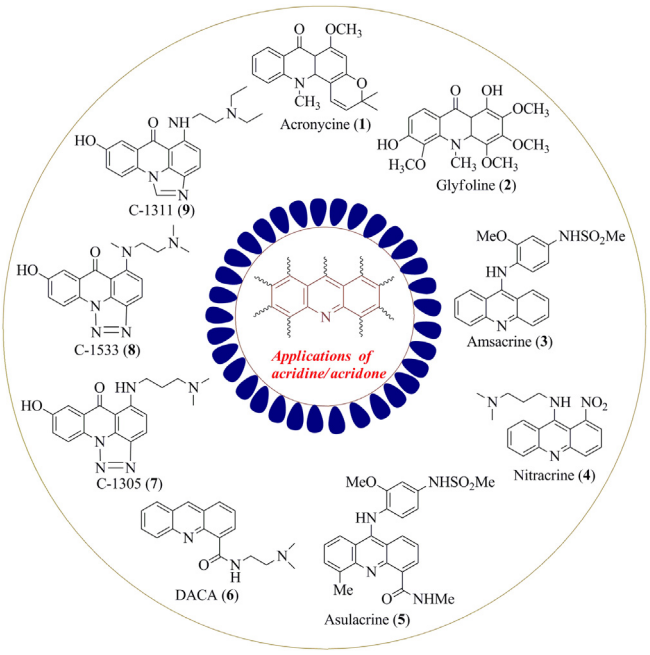

Fig. 1. Chemical structures of biologically important acridine/acridone based derivatives.

imidazoloacridone [20,21], triazoloacridone derivatives, C-1305 (**7**) and C-1533 (**8**), which cause the changes in DNA sequences, of cancer cells, containing guanine triplets [22,23]. On the other hand, imidazoloacridone derivative, C-1311 (**9**), showed its anti-cancer potential through the inhibition of cell cycle in G_2 phase in cancer cells [20,24]. The acridone nucleus have been explored at various positions, but the majority of the N10 substituted acridone derivatives have been reported to possess both anti-cancer and MDR modulator potential [25–28].

In the light of the above, a series of fifteen N10-substituted acridone derivatives, *i.e.* 2-(9-oxoacridin-10(9*H*)-*yl*)-N-phenyl acetamides, was synthesized, and subsequently screened for their *in vitro* anti-cancer activity against three different human cancer cell lines including MCF-7 (Breast cancer), HeLa (cervical) and A-549 (lung adenocarcinoma). In addition to this, the docking simulation was performed to identify the binding pattern of these molecules in the active site of MDR protein and to evaluate their subsequent MDR modulator potential.

2. Result and discussion

2.1. Chemistry

The synthesis of compounds **13a**–**o** was performed as described in Scheme 1, in which the starting material acridone (**10**) was synthesized as reported in the literature [29,30]. The second reactant, 2-chloro-N-phenyl acetamide (**12a**–**o**), subsequently condensed with acridone molecule (**10**), was also synthesized according to the method reported in the literature [31]. These two starting reactants were refluxed in the presence of sodium hydride (NaH) and *N,N*-dimetyl formamide (DMF) resulting in the formation of target compounds **13a**–**o**.

Since the nitrogen of acridone ring is a weak base in nature, the alkylation at N10 position of acridone ring is less favorable. This problem can then be overcome using strong bases, like potassium hydroxide (KOH), sodium hydroxide (NaOH), sodamide ($NaNH_2$) or sodium hydride (NaH), under anhydrous conditions. Previous reports described the alkylation at N10 position of acridone ring in the presence of potassium hydroxide (KOH) using DMF as solvent, where the water content released during the reaction was separated azeotropically [32,33]. The further modification of this reaction was performed using phase transfer catalyst (PTC) benzyltrimethylammonium bromide (BTMAB) in the presence of toluene as solvent; however this reaction was too long due to refluxing of reaction mixture for five days [34]. Thus, to shorten the reaction time period, the reaction mixture was initially refluxed for 10 h in the presence of tetrabutylammonium bromide (TBAB) as PTC, and then worked up with ether and water, and finally recrystallized from ethanol to obtain N-alkylated acridones as a final product [35]. On the other hand, several researchers have reported the synthesis of N10-alkylated acridones in the presence of NaH and DMF, which was actually considered for the synthesis of our 2-(9-oxoacridin-10(9*H*)-*yl*)-N-phenyl acetamide derivatives (**13a**–**o**) [25,36]. The target molecules (**13a**–**o**) were obtained from the condensation reaction of acridone molecule (**10**) with 2-chloro-N-phenylacetamide derivatives (**12a**–**o**). In this reaction, initially acridone molecule (**10**) was treated with NaH in the presence of DMF at 0 °C, to obtain sodium salt of acridone. Further, this sodium salt of acridone was treated with 2-chloro-N-phenylacetamide derivatives (**12a**–**o**) in the presence of potassium iodide (KI), which activates the reaction mixture.

The IR spectra of 2-chloro-N-phenylacetamide derivatives (**12a**–**o**) showed characteristic absorption bands in the region of 1690–1640 cm^{-1} (C═O) due to the presence of –CONH group and secondary amino group showed the –CONH stretching frequency at 3400–3200 cm^{-1}. These peaks confirmed the formation of intermediate compounds (**12a**–**o**). Targeted compounds **13a**–**o** has conjugated ketone (>C═O) at nine position of acridone ring that showed additional peaks at 1650–1600 cm^{-1}. The ^{1}H NMR spectrum of above synthesized compounds showed aromatic protons at '*δ*' 6.00–9.00 ppm, splitting and multiplicity of peaks are being discussed in the experimental section. A broad singlet at '*δ*' 8–10 ppm was assigned to CONH proton of the amide group and singlet at '*δ*' 4.00–5.00 ppm for $NHCOCH_2$ group. A broad singlet at '*δ*' 11.63 ppm was assigned to OH proton (**13h**) and broad singlet at '*δ*' 10–12 ppm was assigned to COOH proton (**13k** and **13l**) of the aromatic carboxylic acid group. All compounds were examined by mass spectroscopy and their molecular mass was determined by $[M]^+$, $[M + 1]^+$, $[M - 1]^+$ and $[M + Na]^+$ peaks. All the IR, ^{1}H NMR and Mass spectral data of compounds was found to be in accordance with assumed structures. The purity of the synthesized compounds was monitored by TLC and ascertained by elemental analysis.

2.2. Biology

The *in vitro* anti-cancer potential of synthesized 2-(9-oxoacridin-10(9*H*)-*yl*)-N-phenyl acetamide derivatives (**13a**–**o**) was determined, using MTT assay, in three different human cancer cell lines including breast (MCF-7), cervical (HeLa), and lung adenocarcinoma (A-549) [37–39]. All *in vitro* anti-cancer screening experiments were repeated in triplicates at five dose levels, and the corresponding results are mentioned in Table 1. With few exceptions, the active analogs showed a remarkable antitumor activity, suggesting that 2-chloro-N-(substituted) phenyl acetamide derivatives could significantly enhance anti-cancer potency. According to the data presented in Table 1, all tested compounds showed a variation in the cytotoxic activity with variation in the substituent on the phenyl ring of the substituent present at the 10th position of acridone nucleus. The unsubstituted molecule **13a,** showed the least activity whereas the substitution with halogen atom such as in molecules **13b**, **13c**, **13m**, **13n** and **13o** showed little improvement in

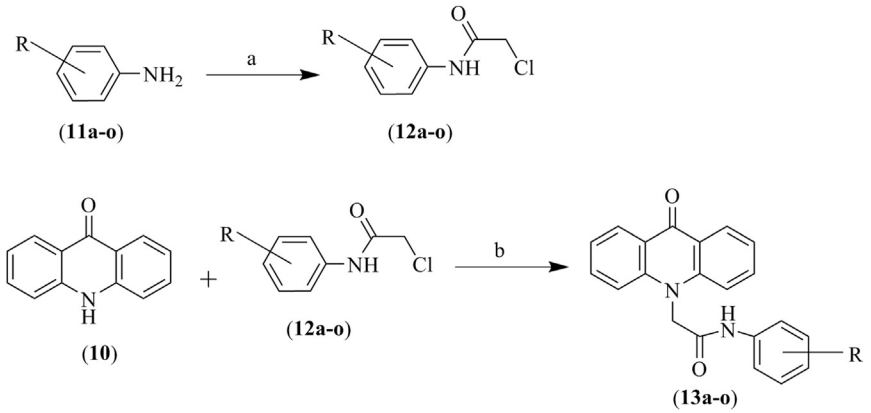

Scheme 1. Schematic diagram for the synthesis of intermediate compounds (**12a**–**o**) and final target compounds (**13a**–**o**). Reagents and conditions: (a) $ClCH_2COCl$, CH_3COOH, CH_3COONa, stirring; (b) NaH, DMF, Reflux.

cytotoxic activity. Compounds containing methyl (**13f**), methoxy (**13g**) and hydroxyl (**13h**) group showed significant improvement of cytotoxic activity. The substitution with nitro group ($-NO_2$) in molecules **13d** and **13e** showed approximately three fold increase in the activity as compared to unsubstituted molecule **13a**. Among all the synthesized compounds, the substitution with carboxylic group (−COOH) at position 2 and 4 of phenyl ring in molecules **13k** and **13l** enhanced two fold cytotoxic activity as compared to molecules **13d** and **13e**.

The data showed that the cell killing potency of tested molecules against MCF-7 and Hela cell lines follows the order **13k** > **13l** > **13d** > **13e** > **13g** > **13h** > **13f** while in the A-549 cell line, potency order is **13k** > **13l** > **13d** > **13g** > **13h** > **13e** > **13f**. Overall, compounds **13k** and **13l** showed highest cytotoxic activity against three cell lines selected for the present study.

2.3. Molecular modeling studies

Anti-cancer drugs have an inherent property of developing the multidrug resistance, which significantly reduces the therapeutic use and effect of chemotherapy. Chemotherapeutics can mediate the MDR primarily by increasing the efflux of cytotoxic drugs from cells through ATP-binding cassette (ABC) transporter proteins, *e.g.,* P-gp. The efflux of drug molecules from cells causes the conformational changes in the transporter persuaded by binding of ATP followed by hydrolysis into ADP. Thus, targeting the inhibition of this hydrolysis process by altering interactions of ATP or Mg^{2+} chelation could aid in blocking P-gp activity. Another approach for blocking P-gp involves the targeting of transmembrane binding pocket.

The acridone nucleus and its derivatives have been reported to modulate multi-drug resistance acting *via* ATP binding and transmembrane domain. To reveal the MDR modulatory activity and binding behavior of the synthesized molecules, molecular docking simulations were carried out. For docking analysis, two reported crystal structures of P-gp, with different binding sites, *i.e.,* ATP binding site (1MV5; 4.4Å; *Lactococcus lactis*) and transmembrane binding pocket (3G60; 3.1Å; *Mus musculus*), were considered to investigate the multi-drug resistance modulatory activity of the compounds. Since the reported crystal structures are from non-human sources, the amino acid sequence of human source (UniProt accession code: P08183) and reported crystal structures 3G60 and 3G5U (Apo-form; 3.8Å; *M. musculus*) were compared in ClustalW online server [40]. During this, all of active site amino acid residues were observed to be conserved exhibiting similar active site environment in sequence of human protein to that of protein for which crystal structure is available. Thus in the absence of the crystal structure of human protein, available structures 3G60 and 1MV5 can be used for docking analysis.

The docking simulations of studied molecules revealed better interactions within the ATP binding pocket as compared to the transmembrane binding pocket. Among all studied molecules, **13i**, **13j**, **13l** and **13n** showed essential hydrogen bonding interactions with the ATP binding pocket amino acid residues (Figs. 2–5). The carbonyl 'O' of acridone ring of these four molecules displayed an essential hydrogen bonding interaction with hydroxyl group of Tyr1393 (O…OH). In case of molecules **13i**, **13l** and **13n**, the benzene ring substituted at the 10^{th} position of acridone rind displayed π−π interactions with Tyr 2352 amino acid residue. In molecules **13j** and **13n**, the NH of amide linker showed hydrogen bonding interaction with carboxylate group of Asp1353 (NH…O) while in molecules **13i** and **13l**, the carbonyl 'O' of the amide linker displayed a hydrogen bonding interaction with the hydroxyl group of Tyr2393 (O…OH). Additionally, in molecule **13l**, the carboxylate group substituted at the benzene ring displayed Mg^{2+} co-ordination. For better understanding, the binding modes of molecules **13i**, **13j**, **13l**, **13n**, and the stereoview of these molecules into the ATP binding site is displayed in Fig. 6. The observed interaction of molecule 13l include important Mg^{2+} coordination, which would reduce ATP hydrolysis. All molecules were docked well into the binding site of protein, consequently they may serve as MDR modulators along with their anti-cancer potential.

2.4. ADME prediction

Determination of ADME properties of synthesized molecules is an essential effort that can avoid failure of candidates in later stages due to the poor pharmacokinetic profile. The '*drug likeness*' of selected synthesized 15 acridone analogs was analyzed by calculating various ADME parameters using '*QikProp*' program of Maestro. The calculated parameters then determine ADME of molecules, *e.g.* partition co-efficient ($QPlogP_{o/w}$), water solubility (QPlogS), cell permeability (QPPCaco) and percentage human oral absorption.

Table 1
Anti-proliferative activity profile of synthesized 2-(9-oxoacridin-10(9*H*)-*yl*)-N-(substituted) phenyl acetamides.

S. No.	R	IC_{50} (μM)[a]		
		MCF-7	HeLa	A-549
13a	H	39.73 ± 0.369	43.77 ± 0.248	41.39 ± 0.313
13b	3-Cl	30.13 ± 0.273	29.05 ± 0.346	33.28 ± 0.288
13c	4-Cl	31.20 ± 0.576	32.28 ± 0.318	34.87 ± 0.569
13d	2-NO_2	12.59 ± 0.842	13.16 ± 0.394	11.84 ± 0.464
13e	4-NO_2	14.00 ± 0.293	17.16 ± 0.348	19.66 ± 0.336
13f	4-CH_3	20.06 ± 0.163	21.90 ± 0.421	20.15 ± 0.432
13g	4-OCH_3	15.01 ± 0.346	19.62 ± 0.329	16.74 ± 0.553
13h	4-OH	15.63 ± 0.232	22.00 ± 0.404	17.44 ± 0.30
13i	4-CF_3	26.39 ± 0.356	23.25 ± 0.394	20.49 ± 0.405
13j	3-CF_3	35.08 ± 0.363	34.87 ± 0.403	38.23 ± 0.345
13k	2-COOH	6.07 ± 0.502	8.80 ± 0.369	7.39 ± 0.356
13l	4-COOH	7.12 ± 0.401	10.66 ± 0.371	8.80 ± 0.612
13m	4-F	27.50 ± 0.380	26.60 ± 0.323	24.54 ± 0.278
13n	2-F	29.24 ± 0.323	25.45 ± 0.308	23.30 ± 0.427
13o	4-Br	33.04 ± 0.402	32.20 ± 0.365	35.15 ± 0.465

[a] Results are expressed as mean percent of MTT absorbance (ratio of absorbance in test compound treated and control cells). Data points represents means of three independent experiments ±SEM, $n = 3$, $p < 0.001$.

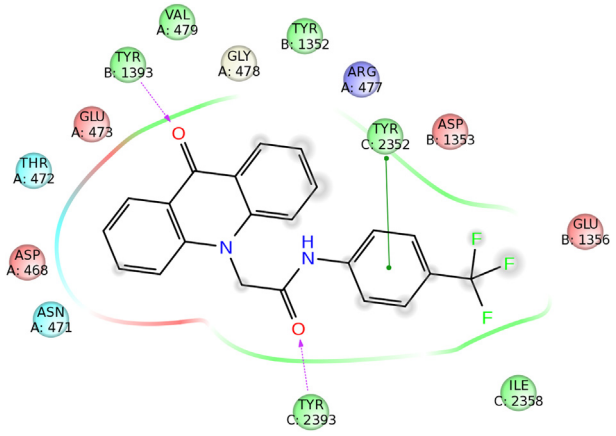

Fig. 2. Binding interactions of molecule **13i** in protein 1MV5.

The calculated ADME parameters of 15 molecules are in acceptable range, *i.e.* QPlog$P_{o/w}$, 2.948 to 4.662; QPlogS, −6.002 to −4.21; QPlogHERG, −6.315 to −4.001; QPPCaco, 46.48 to 2190.691; QPPMDCK, 22.817 to 4543.444 and percentage human oral absorption, 74.119–100%; thus these molecules would be orally active for human use. The calculated parameters of all 15 molecules are mentioned in Table 2.

3. Conclusion

Fifteen new N-10 substituted acridone derivatives have been synthesized and evaluated for cytotoxicity against three cell lines. Most of the compounds showed good inhibiting activity against these cell lines. Compounds **13k**, **13l**, **13d**, **13e** and **13h** bearing electron withdrawing groups like −COOH, $-NO_2$, −OH exhibited good cytotoxic activity as compared to unsubstituted **13a** or compound **13f** bearing electron releasing groups ($-CH_3$). Halogen substitution has little effect on cytotoxicity. The *in vitro* cytotoxicity activity showed that **13k** and **13l** bear good activity against MCF-7, A-549 and HeLa cancer cell lines in the low micromolar range as compared to other compounds. The mechanism of action of these novel leads will be the subject of further studies, aimed at identifying highly potent, safe and selective agents for treatment of cancer. Probably the cytotoxicity is conferred *via* DNA intercalation and further studies to investigate this are in progress.

The computational analysis showed that all molecules display significant interactions with ATP binding site and may act as MDR modulators. On the basis of this analysis, it can be concluded that synthesized compounds showed significant anti-cancer activity in addition to their predicted MDR modulator effects.

4. Experimental section

4.1. Chemistry

All the chemicals and solvents utilized for the synthesis work were purchased from Central Drug House (CDH) Pvt. Ltd., New Delhi and Hi-Media Laboratories Pvt. Ltd, Mumbai. The progress of chemical reactions was monitored by thin layer chromatography (TLC), performed on Merck silica gel 60 F_{254} aluminum sheets, using chloroform: methanol (9:1, *v*/*v*) as developing system (S_1). The detection of sport was performed under UV light. The final products were identified using column chromatography, on silica gel (60–120 mesh size). The melting points of the compounds were determined on a Veego-programmable melting point apparatus (microprocessor based). The IR spectra of the molecules were recorded on FTIR Perkin Elmer two Spectrum. ^{1}H NMR of the molecules was recorded on a Bruker Avance II, 400 MHz spectrophotometer, using tetramethylsilane (TMS) as internal standard. The mass spectra at ESI-MS mode (positive and negative) were recorded with Agilent Technologies 6410 Triple Quad LC/MS. Elemental analysis for the quantitative determination of C, H and N content was carried out in Vario MICRO CUBE Elemental analyzer.

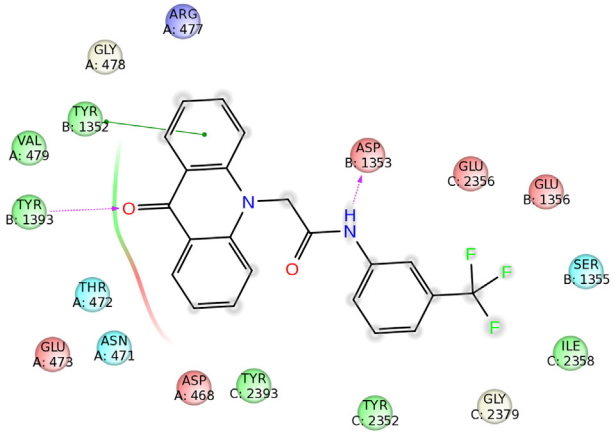

Fig. 3. Binding interactions of molecule **13j** in protein 1MV5.

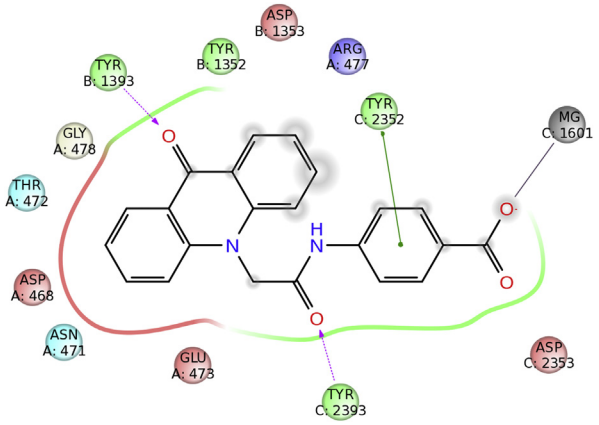

Fig. 4. Binding interactions of molecule **13l** in protein 1MV5.

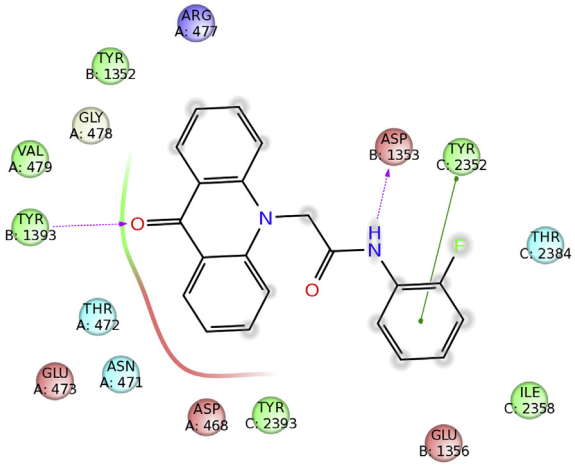

Fig. 5. Binding interactions of molecule **13n** in protein 1MV5.

*4.1.1. General synthetic procedure for 2-chloro-N-(substituted) phenyl acetamides (**12a**–**o**)*

Initially, appropriate amine (0.05 mol) was dissolved in glacial acetic acid (25 ml) containing saturated solution of sodium acetate (25 ml). In case, if the substance did not dissolve completely then the mixture was warmed and the resultant solution was cooled in an ice-bath with stirring. To the ice cold solution chloroacetyl chloride (4.8 ml, 0.06 mol) was added drop wise with continuous stirring to avoid the vigorous reaction. After half an hour, a white colored product was separated out and filtered. The product was firstly washed with 50% aqueous acetic acid and finally with water. The crude product was then recrystallized from ethanol. The product so obtained was dried under vacuum to obtain the series of intermediate compounds (**12a**–**o**).

*4.1.1.1. 2-chloro-N-phenyl acetamide (**12a**).* Yield: 92%; White crystals; m.p: 128–130 °C; IR (KBr, cm^{-1}) 3313.30, 2951.20, 1656.60, 1614.50, 1437.30, 1239.60, 769.70; ^{1}H NMR (400 MHz, $CDCl_3$) δ 8.28 (br s, 1H, NH), 7.55–7.53 (t, J = 6.4 Hz, 2H, Ar-H), 7.37–7.33 (t, J = 15.9 Hz, 2H, Ar-H), 7.18–7.14 (t, J = 14.4 Hz, 1H, Ar-H), 4.17 (s, 2H, CH_2); LC–MS (m/z): positive mode 170.00 $[M]^+$; Anal. Calcd for C_8H_8ClNO (169.61): C, 56.65; H, 4.75; N, 8.26. Found: C, 56.76; H, 4.707; N, 8.18.

*4.1.1.2. 2-chloro-N-(3-chlorophenyl)acetamide (**12b**).* Yield: 94%; White crystals; m.p: 103–105 °C; IR (KBr, cm^{-1}) 3269.20, 3088.50, 2945.60, 1680.30, 1594.50, 1475.60, 1251.20, 780.60; ^{1}H NMR (400 MHz, $CDCl_3$) δ 8.34 (br s, 1H, NH), 7.66–7.65 (t, 1H, Ar-H), 7.40–7.37 (m, 1H, Ar-H) 7.28–7.24 (t, 1H, Ar-H), 7.15–7.12 (m, 1H, Ar-H), 4.17 (s, 2H, CH_2); LC–MS (m/z): positive mode 203.90 $[M]^+$; Anal. Calcd for $C_8H_7Cl_2NO$ (204.05): C, 47.09; H, 3.46; N, 6.86. Found: C, 46.78; H, 3.677; N, 6.76.

*4.1.1.3. 2-chloro-N-(4-chlorophenyl)acetamide (**12c**).* Yield: 88%; White crystals; m.p: 170–172 °C; IR (KBr, cm^{-1}) 3263.20, 3080.90, 2950.70, 1669.50, 1613.20, 1489.90, 1246.50, 775.60; ^{1}H NMR (400 MHz, $CDCl_3$) δ 10.12 (br s, 1H, NH), 7.62–7.58 (m, 2H, Ar-H), 7.27–7.24 (m, 2H, Ar-H), 4.14 (s, 2H, CH_2); LC–MS (m/z): positive mode 204.00 $[M]^+$, 221.20 $[M + Na]^+$; Anal. Calcd for $C_8H_7Cl_2NO$ (204.05): C, 47.09; H, 3.46; N, 6.86. Found: C, 46.78; H, 3.387; N, 6.62.

*4.1.1.4. 2-chloro-N-(2-nitrophenyl)acetamide (**12d**).* Yield: 85%; Yellow crystals; m.p: 96–98 °C; IR (KBr, cm^{-1}) 3307.40, 3018.20, 2961.30, 1688.10, 1607.10, 1511.60, 1338.80, 1276.60, 737.70; ^{1}H NMR (400 MHz, $CDCl_3$) δ 10.95 (br s, 1H, NH), 8.41–8.39 (d, J = 7.92 Hz, 1H, Ar-H), 8.15–8.13 (d, J = 7.88 Hz, 1H, Ar-H), 7.72–7.69 (t, 1H, Ar-H), 7.34–7.31 (t, 1H, Ar-H), 4.32 (s, 2H, CH_2); LC–MS (m/z): negative mode 214.00 $[M - 1]^+$; Anal. Calcd for $C_8H_7ClN_2O_3$ (214.61): C, 44.77; H, 3.29; N, 13.05. Found: C, 45.89; H, 3.250; N, 13.04.

*4.1.1.5. 2-chloro-N-(4-nitrophenyl)acetamide (**12e**).* Yield: 88%; Yellow crystals; m.p: 178–180 °C; IR (KBr, cm^{-1}) 3275.40, 3014.60, 2937.70, 1685.30, 1626.80, 1502.60, 1337.80, 1253.80, 746.90; ^{1}H NMR (400 MHz, $CDCl_3$) δ 12.15 (br s, 1H, NH), 8.67–8.65 (t, J = 3.88 Hz, 1H, Ar-H), 8.10–8.09 (d, J = 4.32 Hz, 1H, Ar-H), 7.55–7.45 (d, J = 3.28 Hz, 1H, Ar-H), 7.15–7.13 (d, J = 7.24 Hz, 1H, Ar-H), 4.20 (s, 2H, CH_2); LC–MS (m/z): negative mode 212.90 $[M - 1]^+$; Anal. Calcd for $C_8H_7ClN_2O_3$ (214.61): C, 44.77; H, 3.29; N, 13.05. Found: C, 45.00; H, 3.250; N, 13.04.

*4.1.1.6. 2-chloro-N-p-(tolyacetamide) (**12f**).* Yield: 84%; White crystals; m.p: 162–164 °C; IR (KBr, cm^{-1}) 3272.20, 3089.40, 2951.80, 1672.50, 1615.80, 1448.20, 1249.70, 715.10; ^{1}H NMR (400 MHz, $CDCl_3$) δ 8.22 (br s, 1H, NH), 7.42–7.40 (d, J = 8.44 Hz, 2H, Ar-H), 7.16–7.14 (d, J = 8.24 Hz, 2H, Ar-H), 4.16 (s, 2H, CH_2), 2.32 (s, 3H, CH_3); LC–MS (m/z): positive mode 184.00 $[M]^+$, 205.90 $[M + Na]^+$; Anal. Calcd for $C_9H_{10}ClNO$ (183.63): C, 58.86; H, 5.49; N, 7.63. Found: C, 58.65; H, 5.336; N, 7.52.

*4.1.1.7. 2-chloro-N-(4-methoxyphenyl)acetamide (**12g**).* Yield: 87%; Gray crystals; m.p: 124–125 °C; IR (KBr, cm^{-1}) 3293.30, 3071.60, 2956.10, 1664.50, 1604.30, 1463.80, 1247.30, 787.60; ^{1}H NMR (400 MHz, $CDCl_3$) δ 9.69 (br s, 1H, NH), 7.52–7.48 (m, 2H, Ar-H), 6.85–6.81 (m, 2H, Ar-H), 4.13 (s, 2H, CH_2), 3.76 (s, 3H, OCH_3); LC–MS (m/z): positive mode 200.00 $[M]^+$, 222.00 $[M + Na]^+$; Anal. Calcd for $C_9H_{10}ClNO_2$ (199.63): C, 54.15; H, 5.05; N, 7.02. Found: C, 54.52; H, 4.982; N, 6.76.

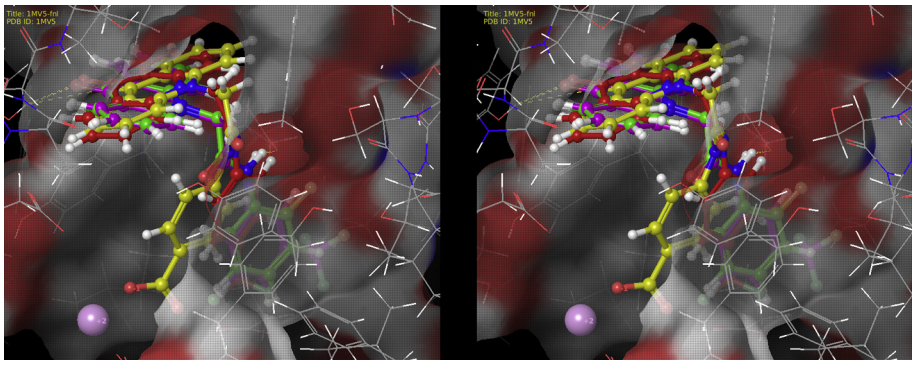

Fig. 6. Stereoview for binding modes of molecules **13i**, **13j**, **13l** and **13n** into ATP binding pocket.

Table 2
ADME properties of 15 synthesized compounds using Qikprop module of Maestro 9.2.

Compound code	QPlog$P_{o/w}$[a]	QPlogS[b]	QPlogHERG[c]	QPPCaco[d]	QPPMDCK[e]	Percent human oral absorption[f]
13a	3.664	−4.545	−6.226	1919.180	1000.840	100
13b	4.156	−5.279	−6.170	1927.001	2484.916	100
13c	4.156	−5.278	−6.170	1928.249	2488.231	100
13d	3.115	−4.314	−5.925	501.745	234.751	93.52
13e	2.951	−4.682	−6.194	232.085	102.021	86.56
13f	3.965	−5.097	−6.168	1927.646	1005.613	100
13g	3.748	−4.700	−6.083	1931.802	1007.956	100
13h	2.948	−4.343	−6.118	575.201	272.109	93.60
13i	4.657	−5.985	−6.240	1929.878	4543.444	100
13j	4.662	−6.002	−6.255	1923.026	4537.730	100
13k	3.614	−4.210	−4.001	133.504	71.376	86.15
13l	2.960	−4.495	−4.398	46.480	22.817	74.12
13m	3.896	−4.900	−6.109	1928.706	1815.423	100
13n	3.883	−4.847	−6.315	2190.691	1576.812	100
13o	4.228	−5.385	−6.201	1928.706	2667.812	100

[a] Predicted octanol/water partition co-efficient log P (acceptable range: −2.0 to 6.5).
[b] Predicted aqueous solubility: S in mol/L (acceptable range: −6.5 to 0.5).
[c] Predicted IC_{50} value for blockage of HERG K^+ channels (concern below −5.0).
[d] Predicted Caco-2 cell permeability in nm/s (acceptable range: <25 is poor and >500 is great).
[e] Predicted apparent MDCK cell permeability in nm/s.
[f] Percentage of human oral absorption (<25% is poor and >80% is high).

*4.1.1.8. 2-chloro-N-(4-hydroxyphenyl)acetamide (**12h**).* Yield: 80%; White crystals; m.p: 138–140 °C; IR (KBr, cm^{-1}) 3436.60, 3275.50, 3104.36, 2940.82, 1684.15, 1622.81, 1597.01, 1256.33, 773.38; ^{1}H NMR (400 MHz, $CDCl_3$) δ 9.35 (s, 1H, OH), 8.92 (br s, 1H, NH), 7.37–7.34 (d, J = 8.84 Hz, 2H, Ar-H), 6.79–6.76 (d, J = 8.88 Hz, 2H, Ar-H), 4.11 (s, 2H, CH_2); LC–MS (m/z): positive mode 186.00 $[M]^+$, 207.90 $[M + Na]^+$; Anal. Calcd for $C_8H_8ClNO_2$ (185.61): C, 51.77; H, 4.34; N, 7.55. Found: C, 51.24; H, 4.506; N, 7.01.

*4.1.1.9. 2-chloro-N-(4-trifluomethylphenyl)acetamide (**12i**).* Yield:84%; White crystals; m.p: 155–156 °C; IR (KBr, cm^{-1}) 3213.20, 3016.20, 2974.10, 1691.60, 1586.50, 1454.00, 1269.60, 1175.10, 753.20; ^{1}H NMR (400 MHz, $CDCl_3$) δ 12.08 (br s, 1H, NH), 8.64–8.62 (d, J = 8.4 Hz, 1H, Ar-H), 8.07–8.05 (d, J = 7.88 Hz, 1H, Ar-H), 7.57–7.53 (t, 1H, Ar-H), 7.17–7.13 (t, 1H, Ar-H), 4.26 (s, 2H, CH_2); LC–MS (m/z): negative mode 235.90 $[M - 1]^+$; Anal. Calcd for $C_9H_7ClF_3NO$ (237.61): C, 45.49; H, 2.97; N, 5.89. Found: C, 45.89; H, 3.029; N, 5.76.

*4.1.1.10. 2-chloro-N-(3-trifluomethylphenyl)acetamide (**12j**).* Yield: 86%; White crystals; m.p: 84–86 °C; IR (KBr, cm^{-1}) 3233.90, 3125.10, 2960.30, 1686.00, 1606.20, 1485.90, 1249.10, 1124.70, 745.10; ^{1}H NMR (400 MHz, $CDCl_3$) δ 8.56 (br s, 1H, NH), 7.84 (s, 1H, Ar-H), 7.74–7.72 (d, J = 7.8 Hz, 1H, Ar-H), 7.46–7.39 (m, 2H, Ar-H), 4.18 (s, 2H, CH_2); LC–MS (m/z): negative mode 235.90 $[M - 1]^+$; Anal. Calcd for $C_9H_7ClF_3NO$ (237.61): C, 45.49; H, 2.97; N, 5.89. Found: C, 45.00; H, 2.803; N, 5.67.

*4.1.1.11. 4-(2-chloroacetamide) benzoic acid (**12k**).* Yield: 85%; White crystals; m.p: 174–176 °C; IR (KBr, cm^{-1}) 3456.50, 3266.10, 3097.10, 2947.40, 1672.20, 1605.10, 1496.8, 1249.20, 750.50; ^{1}H NMR (400 MHz, $CDCl_3$) δ 10.51 (br s, 1H, COOH), 9.35 (br s, 1H, NH), 7.82–7.80 (d, J = 8.52 Hz, 2H, Ar-H), 7.58–7.56 (d, J = 8.6 Hz, 2H, Ar-H), 4.22 (s, 2H, CH_2); LC–MS (m/z): negative mode 211.90 $[M - 1]^+$; Anal. Calcd for $C_9H_8ClNO_3$ (213.62): C, 50.66; H, 3.77; N, 6.56. Found: C, 51.38; H, 4.707; N, 6.31.

*4.1.1.12. 4-(4-chloroacetamide) benzoic acid (**12l**).* Yield: 80%; White crystals; m.p: 250–252 °C; IR (KBr, cm^{-1}) 3444.6, 3268.80, 3084.54, 2922.23, 1672.09, 1614.10, 1491.28, 1248.20, 1192.94, 777.11; ^{1}H NMR (400 MHz, $CDCl_3$) δ 9.75 (br s, 1H, COOH), 8.97 (br s, 1H, NH), 7.38–7.36 (d, J = 8.64 Hz, 2H, Ar-H), 6.74–6.72 (d, J = 8.56 Hz, 2H, Ar-H), 4.11 (s, 2H CH_2); LC–MS (m/z): positive mode 214.00 $[M]^+$; Anal. Calcd for $C_9H_8ClNO_3$ (213.62): C, 50.66; H, 3.77; N, 6.56. Found: C, 50.75; H, 3.853; N, 6.41.

*4.1.1.13. 2-chloro-N-(4-fluorophenyl)acetamide (**12m**).* Yield: 88%; Green crystals; m.p: 130–132 °C; IR (KBr, cm^{-1}) 3311.93, 2919.78, 1654.12, 1615.14, 1436.63, 1261.71, 1111.06, 768.92; ^{1}H NMR (400 MHz, $CDCl_3$) δ 8.41 (br s, 1H, NH), 7.84 (s, 1H, Ar-H), 7.74–7.72 (d, J = 7.8 Hz, 1H, Ar-H), 7.46–7.38 (m, 2H, Ar-H), 4.18 (s, 2H, CH_2); LC–MS (m/z): positive mode 188.00 $[M]^+$; Anal. Calcd for C_8H_7ClFNO (187.60): C, 51.22; H, 3.76; N, 7.47. Found: C, 51.38; H, 3.711; N, 7.43.

*4.1.1.14. 2-chloro-N-(2-fluorophenyl)acetamide (**12n**).* Yield: 84%; White crystals; m.p: 134–136 °C; IR (KBr, cm^{-1}) 3307.42, 2921.59, 1689.49, 1607.86, 1457.27, 1280.42, 1147.16, 770.32; ^{1}H NMR (400 MHz, $CDCl_3$) δ 8.22 (br s, 1H, NH), 7.66–7.65 (t, 1H, Ar-H), 7.40–7.37 (m, 1H, Ar-H), 7.28–7.24 (t, 1H, Ar-H), 7.15–7.12 (m, 1H, Ar-H), 4.17 (s, 2H, CH_2); LC–MS (m/z): positive mode 188.00 $[M]^+$; Anal. Calcd for C_8H_7ClFNO (187.60): C, 51.22; H, 3.76; N, 7.47. Found: C, 51.24; H, 3.705; N, 7.43.

*4.1.1.15. N-(4-bromophenyl)-2-chloroacetamide (**12o**).* Yield: 80%; White crystals; m.p: 180–182 °C; IR (KBr, cm^{-1}) 3211.93, 2919.78, 1672.07, 1593.85, 1419.03, 1219.69, 1042.27, 772.81; ^{1}H NMR (400 MHz, $CDCl_3$) δ 8.99 (br s, 1H, NH), 7.37–7.35 (d, J = 7.96 Hz, 2H, Ar-H), 6.82–6.80 (d, J = 8.36 Hz, 2H, Ar-H), 4.13 (s, 2H, CH_2); LC–MS (m/z): negative mode 247.00 $[M - 1]^+$; Anal. Calcd for $C_8H_7BrClNO$ (248.50): C, 38.67; H, 2.84; N, 5.64. Found: C, 38.65; H, 2.803; N, 5.67.

*4.1.2. General synthetic procedure for 2-(9-oxoacridin-10(9H)-yl)-N-(substituted) phenyl acetamide (**13a–o**)*

Acridone (**10**) (195 mg, 1 mmol) was added portion wise to a stirred suspension of NaH (56 mg, 1.2 mmol, 50% of mineral oil) in dry DMF (10 ml) at 0 °C. The reaction mixture was stirred for 2 h. Afterward, 2-chloro-N-(substituted)phenyl acetamides **12a–o** (2 mmol) and KI (33.2 mg, 0.2 mmol) were added to the reaction mixture with stirring for different time intervals. After completion of the reaction (TLC), the reaction mixture was poured into crushed ice (50 g) with constant stirring. The precipitated solid was

collected and then extracted with chloroform. The combined organic extracts were washed with brine and water and finally dried with anhydrous sodium sulfate. Pure compounds were isolated after column chromatography and recrystallized from suitable solvent.

*4.1.2.1. 2-(9-oxoacridin-10(9H)-yl)-N-phenylacetamide (**13a**).* Yield: 70%; Pale yellow crystals; m.p: 204–205 °C; IR (KBr, cm^{-1}) 3271.73, 3085.40, 2951.35, 1674.68, 1613.46, 1598.24, 1491.60, 1461.22, 1283.13; ^{1}H NMR (400 MHz, DMSO-d_6) δ 10.52 (br s, 1H, NH), 8.42 (d, J = 6.9 Hz, 1H, Ar-H), 8.28 (d, J = 8.3 Hz, 1H, Ar-H), 7.77 (t, J = 7.4 Hz, 1H, Ar-H), 7.66 (t, J = 10.2 Hz, 2H, Ar-H), 7.53 (d, J = 8.4 Hz, 1H, Ar-H), 7.46–7.40 (m, 4H, Ar-H), 7.31 (q, J = 7.7 Hz, 2H, Ar-H), 7.22 (t, J = 7.4 Hz, 1H, Ar-H), 4.52 (s, 2H, CH_2); ^{13}C NMR (400 MHz, DMSO-d_6) δ 176.77, 170.85, 140.86, 138.46, 133.40, 129.44, 128.85, 128.81, 128.77, 128.58, 125.99, 125.19, 123.36, 121.56, 120.95, 120.46, 119.56, 119.33, 119.18, 117.30, 61.86; LC–MS (m/z): negative mode 327.00 $[M-1]^+$; Anal. Calcd for $C_{21}H_{16}N_2O_2$ (328.36): C, 76.81; H, 4.91; N, 8.53. Found: C, 75.09; H, 5.106; N, 8.46.

*4.1.2.2. N-(3-chlorophenyl)-2-(9-oxoacridin-10(9H)-yl)acetamide (**13b**).* Yield: 66%; Yellow crystals; m.p: 220–222 °C; IR (KBr, cm^{-1}) 3271.72, 2948.11, 2849.30, 1681.13, 1613.91, 1595.31, 1478.91, 1429.85, 1253.87, 779.22; ^{1}H NMR (400 MHz, DMSO-d_6) δ 11.64 (br s, 1H, NH), 8.41–8.25 (m, 2H, Ar-H), 7.70–7.66 (m, 3H, Ar-H), 7.46 (ddd, J = 18.9, 10.4, 5.9 Hz, 4H, Ar-H), 7.44–7.21 (m, 3H, Ar-H), 4.49 (s, 2H, CH_2); ^{13}C NMR (400 MHz, DMSO-d_6) δ 176.79, 171.36, 140.86, 139.97, 139.87, 133.35, 133.15, 132.94, 130.47, 130.36, 130.20, 129.42, 126.51, 125.99, 123.05, 120.92, 120.48, 119.06, 117.98, 117.29, 61.89; LC–MS (m/z): negative mode 360.90 $[M-1]^+$; Anal. Calcd for $C_{21}H_{15}ClN_2O_2$ (362.81): C, 69.52; H, 4.17; N, 7.72. Found: C, 69.96; H, 4.095; N, 7.63.

*4.1.2.3. N-(4-chlorophenyl)2-(9-oxoacridine-10(9H)-yl)acetamide (**13c**).* Yield: 60%; Yellow crystals; m.p: 216–218 °C; IR (KBr, cm^{-1}) 3274.23, 3093.49, 2922.28, 1669.53, 1616.30, 1582.21, 1474.28, 1251.44, 797.87; ^{1}H NMR (400 MHz, DMSO-d_6) δ 10.30 (br s, 1H, NH), 8.42–8.08 (m, 1H, Ar-H), 7.64 (dd, J = 15.6, 8.0 Hz, 3H, Ar-H), 7.43–7.30 (m, 5H, Ar-H), 7.28 (d, J = 8.8 Hz, 3H, Ar-H), 4.52 (s, 2H, CH_2); ^{13}C NMR (400 MHz, DMSO-d_6) δ 176.78, 171.10, 140.87, 140.23, 138.81, 137.47, 137.39, 133.36, 130.82, 129.43, 128.74, 128.44, 126.87, 125.99, 121.58, 121.15, 120.93, 120.88, 120.48, 117.29, 61.89; LC–MS (m/z): positive mode 360.90 $[M-1]^+$; Anal. Calcd for $C_{21}H_{15}ClN_2O_2$ (362.81): C, 69.52; H, 4.17; N, 7.72. Found: C, 69.96; H, 4.120; N, 7.63.

*4.1.2.4. N-(2-nitrophenyl)-2-(9-oxoacridin-10(9H)-yl)acetamide (**13d**).* Yield: 65%; Yellowish orange crystals; m.p: 235–237 °C; IR (KBr, cm^{-1}) 3274.52, 2919.74, 2851.09, 1671.59, 1606.40, 1571.52, 1493.88, 1451.53, 1329.73, 1277.49; ^{1}H NMR (400 MHz, DMSO-d_6) δ 10.81 (br s, 1H, NH), 8.27 (d, J = 7.3 Hz, 1H, Ar-H), 8.08 (dd, J = 10.5, 5.7 Hz, 3H, Ar-H), 7.85 (t, J = 7.0 Hz, 1H, Ar-H), 7.74–7.63 (m, 4H, Ar-H), 7.56 (d, J = 8.3 Hz, 1H, Ar-H), 7.37 (t, J = 7.9 Hz, 1H, Ar-H), 7.22 (t, J = 7.1 Hz, 1H, Ar-H), 4.35 (s, 2H, CH_2); ^{13}C NMR (400 MHz, DMSO-d_6) δ 176.76, 171.63, 140.85, 140.15, 135.47, 134.88, 133.38, 132.90, 131.72, 129.45, 125.98, 123.95, 123.40, 122.15, 121.70, 120.94, 120.46, 117.60, 117.29, 111.20, 61.70; LC–MS (m/z): negative mode 371.90 $[M-1]^+$; Anal. Calcd for $C_{21}H_{15}N_3O_4$ (373.36): C, 67.56; H, 4.05; N, 11.25. Found: C, 67.76; H, 3.803; N, 10.72.

*4.1.2.5. N-(4-nitrophenyl)-2-(9-oxoacridin-10(9H)-yl)acetamide (**13e**).* Yield: 72%; Yellowish orange crystals; m.p: 244–245 °C; IR (KBr, cm^{-1}) 3314.66, 3092.05, 2922.98, 1673.18, 1615.12, 1600.00, 1552.75, 1467.19, 1338.21, 1257.58; ^{1}H NMR (400 MHz, DMSO-d_6) δ 10.83 (br s, 1H, NH), 8.31–8.16 (m, 6H, Ar-H), 7.86 (d, J = 9.2 Hz, 2H, Ar-H), 7.76–7.66 (m, 2H, Ar-H), 7.54 (d, J = 8.4 Hz, 1H, Ar-H), 7.22 (t, J = 7.5 Hz, 1H, Ar-H), 4.28 (s, 2H, CH_2); ^{13}C NMR (400 MHz, DMSO-d_6) δ 176.76, 171.64, 140.85, 140.15, 135.47, 133.39, 132.89, 131.72, 129.45, 125.98, 125.57, 125.15, 124.81, 123.96, 123.41, 121.70, 120.95, 120.45, 117.29, 111.20, 61.70; LC–MS (m/z): negative mode 372.00 $[M-1]^+$; Anal. Calcd for $C_{21}H_{15}N_3O_4$ (373.36): C, 67.56; H, 4.05; N, 11.25. Found: C, 67.56; H, 4.095; N, 10.56.

*4.1.2.6. 2-(9-oxoacridin-10(9H)-yl)-N-(p-tolyl)acetamide (**13f**).* Yield: 69%; Yellowish gray crystals; m.p: 228–230 °C; (KBr, cm^{-1}) 3231.43, 2919.63, 2850.55, 1652.42, 1629.17, 1590.93, 1463.52, 1383.83, 1246.92; ^{1}H NMR (400 MHz, DMSO-d_6) δ 10.12 (br s, 1H, NH), 7.73 (ddd, J = 17.2, 11.3, 5.2 Hz, 1H, Ar-H), 7.54–7.46 (m, 3H, Ar-H), 7.25 (dt, J = 12.5, 6.2 Hz, 6H, Ar-H), 7.11 (d, J = 8.3 Hz, 2H, Ar-H), 4.45 (s, 2H, CH_2), 2.28 (s, 3H, CH_3); ^{13}C NMR (400 MHz, DMSO-d_6) δ 176.77, 170.59, 140.87, 136.00, 135.94, 134.10, 133.39, 132.27,128.96, 126.55, 125.99, 125.04, 121.57, 121.01, 120.95, 120.47, 119.54, 119.21, 117.30, 115.84, 61.85, 20.39; LC–MS (m/z): negative mode 341.00 $[M-1]^+$; Anal. Calcd for $C_{22}H_{18}N_2O_2$ (342.39): C, 77.17; H, 5.30; N, 8.18. Found: C, 77.09; H, 5.336; N, 8.18.

*4.1.2.7. N-(4-methoxyphenyl)-2-(9-oxoacridin-10(9H)-yl)acetamide (**13g**).* Yield: 73%; Pale yellow crystals; m.p: 224–226 °C; IR (KBr, cm^{-1}) 3292.23, 2922.60, 2851.95, 1677.33, 1629.83, 1593.99, 1481.16, 1450.47, 1372.12, 1265.11; ^{1}H NMR (400 MHz, DMSO-d_6) δ 10.06 (br s, 1H, NH), 8.42–8.12 (m, 2H, Ar-H), 7.78 (d, J = 13.5 Hz, 1H, Ar-H), 7.54–7.50 (m, 3H, Ar-H), 7.32–7.22 (m, 2H, Ar-H), 6.90 (dd, J = 15.1, 8.2 Hz, 4H, Ar-H), 4.15 (s, 2H, CH_2), 3.75 (s, 3H, OCH_3); ^{13}C NMR (400 MHz, DMSO-d_6) δ 176.79, 170.35, 140.87, 140.27, 133.37, 131.75, 131.60, 129.43, 126.73, 125.99, 123.27, 121.53, 121.14, 120.94, 120.48, 117.30, 114.06, 113.88, 113.67, 111.71, 61.82, 55.06; LC–MS (m/z): positive mode 359.10 $[M]^+$, 381.20 $[M+Na]^+$; Anal. Calcd for $C_{22}H_{18}N_2O_3$ (358.39): C, 73.73; H, 5.06; N, 7.82. Found: C, 73.12; H, 4.911; N, 7.83.

*4.1.2.8. N-(4-hydroxyphenyl)-2-(9-oxoacridin-10(9H)-yl)acetamide (**13h**).* Yield: 64%; Yellow crystals; m.p: 230–232 °C; IR (KBr, cm^{-1}) 3400.53, 3305.98, 2922.84, 2853.30, 1662.65, 1632.02, 1598.18, 1471.22, 1466.08, 1257.79; ^{1}H NMR (400 MHz, DMSO-d_6) δ 11.63 (br s, 1H, OH), 10.57 (br s, 1H, NH), 8.26 (d, J = 7.1 Hz, 2H, Ar-H), 7.70–7.66 (m, 4H, Ar-H), 7.55 (dd, J = 17.4, 8.0 Hz, 2H, Ar-H), 7.31–7.28 (m, 4H, Ar-H), 4.52 (s, 2H, CH_2); ^{13}C NMR (400 MHz, DMSO-d_6) δ 176.76,170.08, 140.85, 133.42, 132.00, 131.31, 130.07, 129.87, 129.45, 125.98, 121.64, 121.35, 121.09, 120.97, 120.45, 117.29, 115.02, 114.93, 114.74, 114.64, 61.76; LC–MS (m/z): positive mode 346.00 $[M+1]^+$; Anal. Calcd for $C_{21}H_{16}N_2O_3$ (344.36): C, 73.24; H, 4.68; N, 8.13. Found: C, 73.12; H, 4.707; N, 8.18.

*4.1.2.9. 2-(9-oxoacridin-10(9H)-yl)-N-(4-(trifluoromethyl) phenyl) acetamide) (**13i**).* Yield: 62%; Yellow crystals; m.p: 248–250 °C; IR (KBr, cm^{-1}) 3267.85, 2920.74, 2850.40, 1671.29, 1626.12, 1599.37, 1434.34, 1243.54, 1120.64; ^{1}H NMR (400 MHz, DMSO-d_6) δ 10.54 (br s, 1H, NH), 8.43–8.09 (m, 1H, Ar-H), 7.84–7.80 (m, 2H, Ar-H), 7.75 (d, J = 8.6 Hz, 3H, Ar-H), 7.66 (d, J = 8.4 Hz, 3H, Ar-H), 7.56 (dd, J = 26.5, 8.5 Hz, 3H, Ar-H), 4.22 (s, 2H, CH_2); ^{13}C NMR (400 MHz, DMSO-d_6) δ 176.82, 171.59, 164.31, 140.88, 140.62, 139.29, 139.21, 133.29, 129.98, 129.71, 129.64, 129.39, 128.88, 125.97, 123.11, 122.11, 122.07, 121.61, 120.86, 120.49, 117.27, 61.89; LC–MS (m/z): positive mode 397.10 $[M+1]^+$; Anal. Calcd for $C_{22}H_{15}F_3N_2O_2$ (396.36): C, 66.67; H, 3.81; N, 7.07. Found: C, 66.66; H, 3.803; N, 7.01.

*4.1.2.10. 2-(9-oxoacridin-10(9H)-yl)-N-(3-(trifluoromethyl)phenyl) acetamide (**13j**).* Yield: 65%; Yellow crystals; m.p: 210–212 °C; IR (KBr, cm^{-1}) 3300.90, 2920.83, 2851.05, 1671.01, 1629.15, 1597.36, 1492.07, 1465.28, 1245.18, 1124.16; ^{1}H NMR (400 MHz, DMSO-d_6) δ 10.58 (br s, 1H, NH), 8.06 (s, 1H, Ar-H), 7.84–7.69 (m, 3H, Ar-H),

7.68–7.61 (m, 6H, Ar-H), 7.55–7.52 (m, 1H, Ar-H), 7.51–7.34 (m, 1H, Ar-H), 4.25 (s, 2H, CH_2); ^{13}C NMR (400 MHz, DMSO-d_6) δ 176.83, 171.59, 164.32, 140.88, 140.62, 139.30, 139.22, 133.26, 129.73, 129.62, 129.41, 128.86, 125.97, 125.17, 123.28, 123.10, 122.10, 122.06, 120.84, 120.50, 117.26, 61.90; LC–MS (m/z): negative mode 395.00 $[M-1]^+$; Anal. Calcd for $C_{22}H_{15}F_3N_2O_2$ (396.36): C, 66.67; H, 3.81; N, 7.07. Found: C, 66.66; H, 3.795; N, 7.01.

*4.1.2.11. 2-(2-(9-oxoacridin-10(9H)-yl)acetamido)benzoic acid (**13k**).* Yield: 62%; Pale yellow solid; m.p: 260–262 °C; IR (KBr, cm^{-1}) 3400.69, 3275.98, 2923.26, 2852.58, 1674.98, 1630.20, 1595.72, 1470.61, 1246.50; ^{1}H NMR (400 MHz, DMSO-d_6) δ 11.57 (br s, 1H, OH), 10.19 (br s, 1H, NH), 8.67 (d, $J = 8.5$ Hz, 1H, Ar-H), 8.36 (dd, $J = 14.3$, 7.2 Hz, 2H, Ar-H), 8.01 (dd, $J = 20.4$, 7.3 Hz, 2H, Ar-H), 7.69–7.61 (m, 5H, Ar-H), 7.34–7.26 (m, 2H, Ar-H), 4.34 (s, 2H, CH_2); ^{13}C NMR (400 MHz, DMSO-d_6) δ 176.82, 171.59, 164.31, 140.88, 140.62, 139.29, 133.29, 129.98, 129.71, 128.88, 125.97, 125.17, 123.11, 122.85, 121.61, 120.86, 120.49, 117.27, 115.77, 115.43, 115.39, 61.89; LC–MS (m/z): positive mode 373.20 $[M+1]^+$; Anal. Calcd for $C_{22}H_{16}N_2O_4$ (372.37): C, 70.96; H, 4.33; N, 7.52. Found: C, 70.97; H, 4.246; N, 7.52.

*4.1.2.12. 4-(2-(9-oxoacridin-10(9H)-yl)acetamido)benzoic acid (**13l**).* Yield: 60%; Pale yellow solid; m.p: 265–267 °C; IR (KBr, cm^{-1}) 3435.03, 3305.98, 2920.40, 2850.78, 1677.58, 1633.08, 1597.68, 1470.62, 1431.39, 1240.86; ^{1}H NMR (400 MHz, DMSO-d_6) δ 11.53 (br s, 1H, OH), 10.36 (br s, 1H, NH), 7.68–7.62 (m, 3H, Ar-H), 7.56–7.49 (m, 3H, Ar-H), 7.31 (t, $J = 9.5$ Hz, 3H, Ar-H), 6.96 (d, $J = 8.9$ Hz, 2H, Ar-H), 6.85–6.83 (m, 1H, Ar-H), 4.44 (s, 2H, CH_2); ^{13}C NMR (400 MHz, DMSO-d_6) δ 176.83, 171.59, 164.32, 140.88, 140.62, 139.30, 133.26, 129.96, 129.73, 129.62, 128.86, 125.97, 125.17, 123.09, 121.61, 120.84, 120.50, 117.26, 115.74, 115.43, 115.39, 61.90; LC–MS (m/z): positive mode 373.10 $[M+1]^+$; Anal. Calcd for $C_{22}H_{16}N_2O_4$ (372.37): C, 70.96; H, 4.33; N, 7.52. Found: C, 70.97; H, 4.413; N, 7.52.

*4.1.2.13. N-(4-fluorophenyl)-2-(9-oxoacridin-10(9H)-yl)acetamide (**13m**).* Yield: 74%; Yellow crystals; m.p: 214–216 °C; IR (KBr, cm^{-1}) 3305.70, 2923.11, 2849.30, 1655.49, 1630.14, 1609.61, 1471.58, 1411.53, 1250.68, 1156.77; ^{1}H NMR (400 MHz, DMSO-d_6) δ 10.41 (br s, 1H, NH), 8.27–8.19 (m, 2H, Ar-H), 7.83–7.65 (m, 3H, Ar-H), 7.54–7.43 (m, 4H, Ar-H), 7.33 (ddd, $J = 16.2$, 13.3, 8.2 Hz, 3H, Ar-H), 4.54 (s, 2H, CH_2); ^{13}C NMR (400 MHz, DMSO-d_6) δ 176.76, 170.81, 140.86, 140.24, 134.90, 134.87, 133.39, 129.44, 127.58, 127.49, 125.98, 121.43, 121.35, 120.94, 120.46, 117.30, 115.51, 115.46, 115.19, 114.97, 61.82; LC–MS (m/z): negative mode 346.90 $[M]^+$; Anal. Calcd for $C_{21}H_{15}FN_2O_2$ (346.35): C, 72.82; H, 4.37; N, 8.09. Found: C, 72.44; H, 4.246; N, 8.07.

*4.1.2.14. N-(2-fluorophenyl)-2-(9-oxoacridin-10(9H)-yl)acetamide (**13n**).* Yield: 72%; Yellow crystals; m.p: 238–240 °C; IR (KBr, cm^{-1}) 3292.44, 2919.85, 2849.30, 1655.59, 1630.32, 1598.63, 1494.48, 1463.01, 1250.54, 1179.94; ^{1}H NMR (400 MHz, DMSO-d_6) δ 10.31 (br s, 1H, NH), 8.45–8.29 (m, 1H, Ar-H), 7.83–7.74 (m, 1H, Ar-H), 7.67–7.59 (m, 1H, Ar-H), 7.53–7.41 (m, 4H, Ar-H), 7.35–7.20 (m, 4H, Ar-H), 7.06 (dd, $J = 7.9$, 1.2 Hz, 1H, Ar-H), 4.55 (s, 2H, CH_2); ^{13}C NMR (400 MHz, DMSO-d_6) δ 176.75, 170.81, 140.86, 140.24, 134.90, 133.41, 129.45, 127.59, 127.51, 125.98, 121.57, 121.42, 121.35, 120.96, 120.45, 117.30, 115.53, 115.47, 115.20, 114.98, 61.81; LC–MS (m/z): negative mode 346.90 $[M]^+$; Anal. Calcd for $C_{21}H_{15}FN_2O_2$ (346.35): C, 72.82; H, 4.37; N, 8.09. Found: C, 72.74; H, 4.413; N, 8.07.

*4.1.2.15. N-(4-bromophenyl)-2-(9-oxoacridin-10(9H)-yl)acetamide (**13o**).* Yield: 65%; Yellow crystals; m.p: 256–258 °C; IR (KBr, cm^{-1}) 3294.51, 2922.29, 2851.89, 1676.69, 1629.42, 1594.06, 1481.03, 1450.25, 1250.14, 1036.62; ^{1}H NMR (400 MHz, DMSO-d_6) δ 11.64 (br s, 1H, NH), 8.27–8.25 (m, 2H, Ar-H), 7.70–7.66 (m, 2H, Ar-H), 7.47 (ddd, $J = 18.9$, 10.4, 5.9 Hz, 4H, Ar-H), 7.25–7.20 (m, 4H, Ar-H), 4.49 (s, 2H, CH_2); ^{13}C NMR (400 MHz, DMSO-d_6) δ 176.76, 171.09, 140.86, 140.23, 138.82, 133.38, 130.81, 129.44, 128.75, 128.73, 128.66, 128.45, 126.97, 126.90, 125.98, 121.59, 121.14, 120.94, 120.47, 117.30, 61.88; LC–MS (m/z): positive mode 408.70 $[M+1]^+$; Anal. Calcd for $C_{21}H_{15}BrN_2O_2$ (407.26): C, 61.93; H, 3.71; N, 6.88. Found: C, 61.89; H, 3.711; N, 6.76.

4.2. Biology

4.2.1. Cell lines and culture medium

Required human cancer cell lines MCF-7 (Breast cancer), HeLa (cervical), and A-549 (lung adenocarcinoma) were procured from National Centre for Cell Sciences (NCCS), Pune, India. Stock cells were cultured in DMEM supplemented with 10% inactivated Fetal Bovine Serum (FBS), penicillin (100 IU/ml), streptomycin (100 μg/ml) and amphotericin B (5 μg/ml) in a humidified atmosphere of 5% CO_2 at 37 °C until confluent. The cells were dissociated with a TPVG solution (0.2% trypsin, 0.02% EDTA, 0.05% glucose in PBS). The stock cultures were grown in 25 cm^2 culture flasks, and all experiments were carried out in 96 microtitre plates.

4.2.2. Cytotoxicity assay

In the each well of the 96 well microtitre plate, 0.1 ml of the diluted cell suspension (approximately 10,000 cells) was added. After 24 h, when a partial monolayer was formed, the supernatant was flicked off, and the monolayer was washed with medium. Then, 100 μl of different test concentrations of test drugs was added on to the partial monolayer in microtitre plates. The plates were then incubated at 37 °C for 3 days in 5% CO_2 atmosphere and microscopic examination was carried out. The observations were noted after an interval of every 24 h. After 72 h, the drug solutions in the wells were discarded, and 50 μl of 3-(4,5-dimethyl thiazol-2-yl)-5-diphenyl tetrazolium bromide (MTT) in PBS, was added to each well. The plates were gently shaken, and incubated for 3 h at 37 °C in 5% CO_2 atmosphere. The supernatant was removed and 100 μl of propanol was added. Subsequently, the plates were gently shaken to solubilize the formed formazan. The absorbance (A) was measured using a microplate reader at a wavelength of 540 nm. The percentage growth inhibition was calculated, and concentration of test compound needed to inhibit cell growth by 50% (IC_{50}) values is generated from the dose–response curves for each cell line. Each experiment was done in triplicate and results are expressed as means ± SEM for each determination. Inhibition was statistically significant compared to that of the control (Student's t-test; $P < 0.001$). IC_{50} values were obtained by nonlinear regression. The following formula was used for the calculation of the percentage of cell viability (CV): CV (%) = (A of the individual test group/A of the control group) × 100.

4.3. Molecular modeling

The sketching and geometry optimization of all molecules was performed in Maestro molecular modeling workspace followed by energy minimization in '*ligprep*' program of Schrödinger software using OPLS_2005 force field at pH of 7.4. The least energy conformations of these molecules were generated in MacroModel program using '*systematic torsion sampling*' algorithm coupled with OPLS_2005 force field.

For the docking analysis, two protein structures 1MV5 and 3G60 [40] were downloaded and optimized. The protein optimization protocol includes the addition of hydrogen atoms, deletion of water molecules, completion of bond orders, assignment of hydrogen bonds and protein ligand complex minimization to RMSD of 0.20Å using OPLS_2005 force field. The active sites of proteins were defined as 10Å around the co-crystal ligand, and then all molecules were docked using extra precision (XP) docking mode of '*glide*' program.

Declaration of interest

The authors report no conflicts of interest.

Contribution

Dr. Om Silakari is an Assistant Professor in the Department of Pharmaceutical Sciences and Drug Research, Punjabi University, Patiala. He designed and supervised whole study. He also helped by his valuable suggestions during work and editing of the manuscript.

Rajesh Kumar is a Ph. D Research Scholar in the Department of Pharmaceutical Sciences and Drug Research, Punjabi University, Patiala. He performed all synthetic work incorporated into the manuscript.

Malkeet Singh Bahia and **Maninder Kaur** is a Ph.D. research scholar. Both performed all the computational work and write down computational results for the manuscript.

Acknowledgments

The authors thank the Principal, Shivalik College of Pharmacy for providing Infrastructure for the synthesis of compounds, Radiant Research Services Pvt. Ltd. Bangalore for evaluating the synthesized compounds for cancer cell cytotoxic studies, Sophisticated Analytical Instruments Facility (SAIF), Panjab University, Chandigarh and Indian Institute of Integrative Medicine (IIIM), Jammu, India for spectral analysis.

Appendix A. Supplementary data

Supplementary data related to this article can be found at http://dx.doi.org/10.1016/j.ejmech.2014.04.030.

References

[1] P.B. Bach, J.R. Jett, U. Pastorino, M.S. Tockman, S.J. Swensen, C.B. Begg, Computed tomography screening and lung cancer outcomes, JAMA 297 (2007) 953–961.
[2] C. Atalay, Multi-drug resistance and cancer, Expert Opinion on Therapeutic Patents 17 (2007) 511–520.
[3] D.J. Harrison, Molecular mechanisms of drug resistance in tumours, Journal of Pathology 175 (1995) 7–12.
[4] H. Thomas, H.M. Coley, Overcoming multidrug resistance in cancer: an update on the clinical strategy of inhibiting P-glycoprotein, Cancer Control 10 (2003) 159–165.
[5] M.M. Gottesman, J. Ludwig, D. Xia, G. Szakacs, Defeating drug resistance in cancer, Discovery Medicine 6 (2006) 18–23.
[6] F.E. Koehn, G.T. Carter, The evolving role of natural products in drug discovery, Nature Reviews Drug Discovery 4 (2005) 206–220.
[7] Y. Liao, Y. Hu, J. Wu, Q. Zhu, M. Donovan, R. Fathi, Z. Yang, Diversity oriented synthesis and branching reaction pathway to generate natural product-like compounds, Current Medicinal Chemistry 10 (2003) 2285–2316.
[8] R. Breinbauer, I.R. Vetter, H. Waldmann, From protein domains to drug candidates-natural products as guiding principles in the design and synthesis of compound libraries, Angewandte Chemie 41 (2002) 2879–2890.
[9] Q.C. Nguyen, T.T. Nguyen, R. Yougnia, T. Gaslonde, H. Dufat, S. Michel, F. Tillequin, Acronycine derivatives: a promising series of anticancer agents, Anti-Cancer Agents in Medicinal Chemistry 9 (2009) 804–815.
[10] T.L. Su, B. Köhler, T.C. Chou, M.W. Chun, K.A. Watanabe, Synthesis of the acridone alkaloids glyfoline and congeners. Structure-activity relationship studies of cytotoxic acridones, Journal of Medicinal Chemistry 35 (1992) 2703–2710.
[11] P. Belmont, J. Bosson, T. Godet, M. Tiano, Acridine and acridone derivatives, anticancer properties and synthetic methods: where are we now? Anti-Cancer Agents in Medicinal Chemistry 7 (2007) 139–169.
[12] P. Belmont, I. Dorange, Acridine/acridone: a simple scaffold with a wide range of application in oncology, Expert Opinion on Therapeutic Patents 18 (2008) 1211–1224.
[13] G. Cholewiński, K. Dzierzbicka, A.M. Kołodziejczyk, Natural and synthetic acridines/acridones as antitumor agents: their biological activities and methods of synthesis, Pharmacological Reports 63 (2011) 305–336.
[14] W.A. Denny, Acridine derivatives as chemotherapeutic agents, Current Medicinal Chemistry 9 (2002) 1655–1665.
[15] T. Bentin, P.E. Nielsen, Superior duplex DNA strand invasion by acridine conjugated peptide nucleic acids, Journal of the American Chemical Society 125 (2003) 6378–6379.
[16] G.J. Atwell, B.F. Cain, R.N. Seelye, Potential antitumor agents. 12. 9-anilinoacridines, Journal of Medicinal Chemistry 15 (1972) 611–615.
[17] G.W. Rewcastle, G.J. Atwell, D. Chambers, B.C. Baguley, W.A. Denny, Potential antitumor agents. 46. Structure-activity relationships for acridine mono-substituted derivatives of the antitumor agent N-[2-(dimethylamino)ethyl]-9-aminoacridine-4-carboxamide, Journal of Medicinal Chemistry 29 (1986) 472–477.
[18] B.C. Baguley, DNA intercalating anti-tumor agents, Anti-Cancer Drug Design 6 (1991) 1–35.
[19] W.M. Cholody, S. Martelli, J. Konopa, 8-substituted 5-[(aminoalkyl)amino]-6*H*-*v*-triazolo[4,5,1-*de*]acridin-6-ones as potential antineoplastic agents. Synthesis and biological activity, Journal of Medicinal Chemistry 33 (1990) 2852–2856.
[20] W.M. Cholody, S. Martelli, J. Paradziej-Luckowicz, J. Konopa, 5-[(aminoalkyl) amino]-imidazolo[4,5,1-*de*]acridin-6-ones as a novel class of antineoplastic agents. Synthesis and biological activity, Journal of Medicinal Chemistry 33 (1990) 49–52.
[21] W.M. Cholody, S. Martelli, J. Konopa, Chromophore-modified antineoplastic imidazoloacridinones. Synthesis and activity against murine leukemias, Journal of Medicinal Chemistry 35 (1992) 378–382.
[22] J. Wesierska-Gadek, D. Schloffer, M. Gueorguieva, M. Uhl, A. Skladanowski, Increased susceptibility of poly(ADP-ribose) polymerase-1 knockout cells to antitumor triazoloacridone C-1305 is associated with permanent G2 cell cycle arrest, Cancer Research 64 (2004) 4487–4497.
[23] K. Lemke, M. Wojciechowski, W. Laine, C. Bailly, P. .Colson, M. Baginski, A.K. Larsen, A. Skladanowski, Induction of unique structural changes in guanine-rich DNA regions by the triazoloacridone C-1305, a topoisomerase II inhibitor with antitumor activities, Nucleic Acids Research 33 (2005) 6034–6047.
[24] Z. Mazerska, P. Sowinski, J. Konopa, Molecular mechanism of the enzymatic oxidation investigated for imidazoacridinone antitumor drug, C-1311, Biochemical Pharmacology 66 (2003) 1727–1736.
[25] C. Gao, Y. Jiang, C. Tan, X. Zu, H. Liu, D. Cao, Synthesis and potent antileukemic activities of 10-benzyl-9 (10H)-acridinones, Bioorganic & Medicinal Chemistry 16 (2008) 8670–8675.
[26] V.S. Gopinath, P. Thimmaiah, K.N. Thimmaiah, Acridones circumvent P-glycoprotein-associated multidrug resistance (MDR) in cancer cells, Bioorganic & Medicinal Chemistry 16 (2008) 474–487.
[27] Y.C. Mayur, Zaheeruddin, G.J. Peters, C. Lemos, L. Kathmann, V.V.S. Rajendra Prasad, Synthesis of 2-fluoro N10-substituted acridones and their cytotoxicity studies in sensitive and resistant cancer cell lines and their DNA intercalation studies, Archiv der Pharmazie – Chemistry in Life Sciences 342 (2009) 640–650.
[28] V.V.S. Rajendra Prasad, G.J. Peters, C. Lemos, I. Kathmann, Y.C. Mayur, Cytotoxicity studies of some novel fluoro acridone derivatives against sensitive and resistant cancer cell lines and their mechanistic studies, European Journal of Pharmaceutical Sciences 43 (2011) 217–224.
[29] C.F.H. Allen, G.H.W. Mckee, Acridone, Organic Syntheses 2 (1943) 15–17.
[30] P. Singh, J. Kaur, B. Yadav, S.S. Komath, Design, synthesis and evaluations of acridone derivatives using Candida albicans-search for MDR modulators led to the identification of an anti-candidiasis agent, Bioorganic & Medicinal Chemistry 17 (2009) 3973–3979.
[31] S.R. Pattan, M. Shamrez Ali, J.S. Pattan, S.S. Purohit, V.V.K. Reddy, B.R. Nataraj, Synthesis and microbiological evaluation of 2-acetanilido-4-arylthiazole derivatives, Indian Journal of Chemistry 45B (2006) 1929–1932.
[32] I.D. Postescu, D. Suciu, A method for N-alkylation of acridones, Journal für Praktische Chemie 318 (1976) 515–518.
[33] I.D. Postescu, G.H. Csavassy, Synthesis and bromination of N-(2-phenylthiazol-4- yl-methyl)-acridone, Journal für Praktische Chemie 319 (1977) 347–352.
[34] J.P. Galy, J. Elguero, E.J. Vincent, A convenient synthesis of N-alkyl acridanones using phase transfer catalysis, Synthesis (2008) 944–946.
[35] K. Papadopoulos, J. Nikokavouras, Synthesis of NN′-dialkyl-9,9′-biacridylidenes and 9,9′-biacridinium nitrates containing long alkyl chains, Journal für Praktische Chemie 335 (1993) 633–636.
[36] V. Hernandez-Olmos, A. Abdelrahman, A. El-Tayeb, D. Freudendahl, S. Weinhausen, C.E. Müller, N-substituted phenoxazine and acridone derivatives: structure-activity relationships of potent P2X4 receptor antagonists, Journal of Medicinal Chemistry 55 (2012) 9576–9588.
[37] T. Mosmann, Rapid colorimetric assay for cellular growth and survival application to proliferation and cytotoxicity assay, Journal of Immunological Methods 65 (1983) 55–63.
[38] F. Denizot, R. Lang, Rapid colorimetric assay for cell growth and survival. modifications to the tetrazolium dye procedure giving improved sensitivity and reliability, Journal of Immunological Methods 89 (1986) 271–277.
[39] Y.Y. Wang, X.X. Zheng, A flow cytometry-based assay for quantitative analysis of cellular proliferation and cytotoxicity in vitro, Journal of Immunological Methods 268 (2002) 179–188.
[40] S.G. Aller, J. Yu, A. Ward, Y. Weng, S. Chittaboina, R. Zhuo, P.M. Harrell, Y.T. Trinh, Q. Zhang, I.L. Urbatsch, G. Chang, Structure of P-glycoprotein reveals a molecular basis for poly-specific drug binding, Science 323 (2009) 1718–1722.